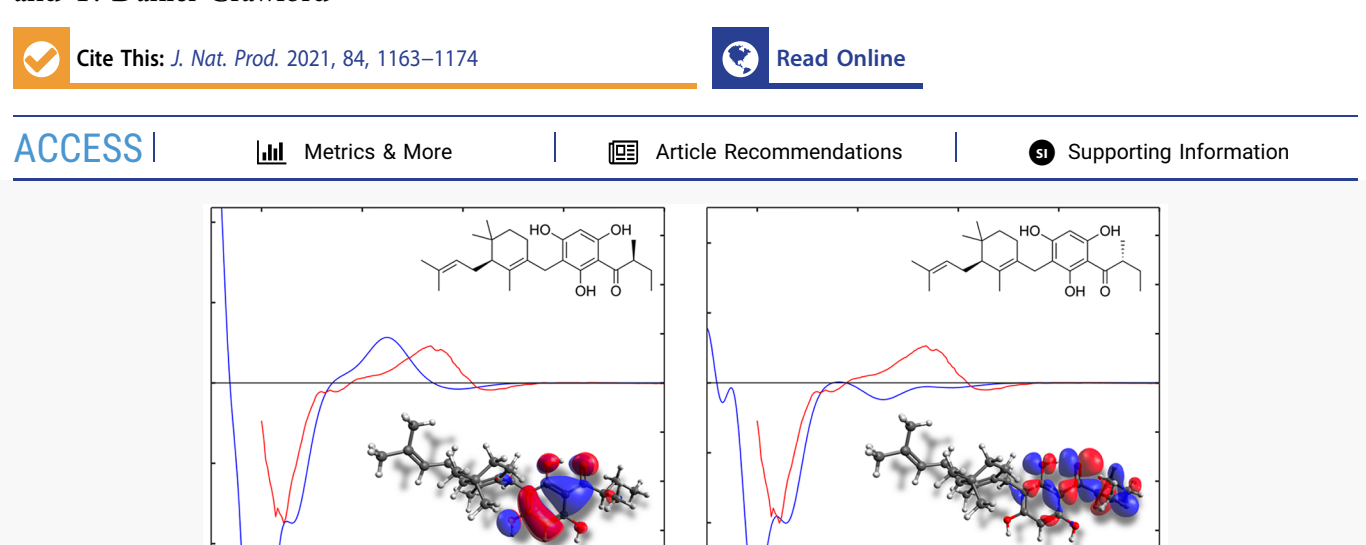


pubs.acs.org/jnp Article

Structure Elucidation and Confirmation of Phloroglucinols from the Roots of *Garcinia dauphinensis* by Comparison of Experimental and Calculated ECD Spectra and Specific Rotations

Kirk C. Pearce, Rolly G. Fuentes, Susana Calderon, Rageshwari Marolikar, David G. I. Kingston, and T. Daniel Crawford*



ABSTRACT: Eight phloroglucinols from *Garcinia dauphinensis* were recently reported to have good to moderate antiplasmodial and anticancer activities, consistent with other phloroglucinol derivatives isolated from natural sources. Chiroptical properties were previously calculated and compared to experimental data for compound 2 as a means to deduce its absolute configuration. Tentative assignments for the remaining compounds were also reported based on these data. In order to arrive at stereochemical assignments for phloroglucinols 1 and 3–8, ECD spectra and specific rotations were computed for all stereoisomers of each compound. Molecular orbital analyses were also carried out for the most energetically favorable conformers of each compound. Absolute configurations are reported for all eight phloroglucinols for the first time.

atural products are incredibly important candidates in the drug discovery process. Owing to their common inherent biological activity, natural products are frequently used as traditional medicine to treat common illnesses and diseases.² Moreover, many pharmaceutical drugs are derived from or inspired by natural products.3 As a result, numerous classes of natural products have been explored extensively for possible therapeutic benefits including sesquiterpenoids, flavonoids, 5,6 xanthones, and phloroglucinols, among others. Although procedures have been developed to consistently isolate enantiomerically pure samples, the assignment of absolute configurations poses a much larger task, especially when the molecules of interest exhibit numerous stereogenic centers. The most convincing experimental approaches rely on X-ray crystallography provided a suitable crystal is available or asymmetric synthesis for noncrystalline compounds. When these methods fail, less reliable chiroptical and NMR techniques are employed. However, the aforementioned experimental methods have varying levels of success, and each of them is subject to certain limitations.

An alternative approach is to compute, directly, the chiroptical properties of selected molecular structures and subsequently compare the results with the associated experimental data of the original compound. Of More specifically, specific rotations and electronic circular dichroism (ECD) spectra are routinely calculated and directly compared to experimental results in an attempt to assign absolute configurations to natural products. It is also well understood that chiroptical properties, more so than others, can be extremely sensitive to small changes in three-dimensional structure (particularly small specific rotations, which are problematic for configuration assignment. In particular, the spatial arrangement of atoms near chromophoric regions becomes increasingly important when modeling ECD

Received: November 14, 2020 Published: April 6, 2021





and specific rotation. As a result, it is essential to thoroughly sample the conformational space to include contributions from all significantly populated conformations. Moreover, if the compound of interest does not have at least a relative configuration secured, this conformational sampling needs to be carried out for every possible stereoisomer. Consequently, molecules that exhibit multiple stereocenters and a high level of flexibility can quickly become computationally prohibitive.

This was undoubtedly the case for phloroglucinols 1–8 which were recently isolated from *Garcinia dauphinensis*, in which an initial conformational search resulted in more than 26 000 conformers to consider.²⁷ As such, the authors elected to focus initial computational studies on 2 as a representative compound. This choice seemed appropriate given the fact that 2 shared identical stereocenters at C-4′ and C-2″ with other compounds, and therefore, tentative assignments about the remaining compounds could be made on the basis that a particular plant will typically only produce one stereochemical series.

The relative configuration of compound 2 at C-2′ and C-4′ was first established by comparing calculated internuclear distances to an experimental NOESY spectrum. Owing to a lack of observed correlation between H-2′ and H-4′, it was determined that 2 depicted an *anti* relative configuration at the left-most stereocenters. In order to determine the absolute configuration, ECD and specific rotations were calculated for all possible stereoisomers according to the procedure described below. The experimental and calculated specific rotations (-16.0 and -47.8° dm $^{-1}$ (g/mL) $^{-1}$, respectively) and ECD spectra (Figure 1) suggested that the best match was for the (R, S, S) stereoisomer (the shorthand stereochemical descriptors refer to C-2′, C-4′, and C-2″, respectively). Based on these data, compound 2 was identified as (2′R, 4′S, 2″S)-4-{[5′,5′-dimethyl-4′-(3-methylbut-2-en-1-yl)-3′-

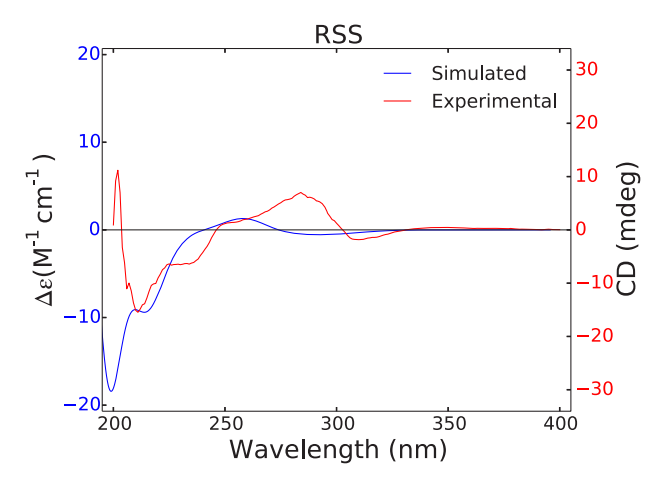


Figure 1. ECD spectrum of compound 2.

 $methylenecyclohexyl] methyl\} - 2 - (2'' - methylbutanoyl) - phloroglucinol. \\^{27}$

As mentioned previously, it is often the case that multiple isolates from a specific natural source will exhibit the same configuration at shared stereocenters. Because phloroglucinols 1-8 all share an identical stereocenter in their 2methylbutanoyl side chain, the remaining compounds were all tentatively assigned an (S) configuration at the common stereogenic center. Moreover, 1 shares an additional stereogenic center with 2, and thus, a tentative (S) configuration at C-4' was assigned in a similar manner. As further evidence of this, the experimental ECD spectra of compounds 1-4 and 6-8 (reported previously by Fuentes et al.²⁷) all showed positive Cotton effects between 285 and 300 nm, which was consistent with a UV absorption of 292 nm for the acylphloroglucinol chromophore,²⁸ suggesting that this effect can be attributed to the 2-methylbutanoylphloroglucinol chromophore. As such, it is worth examining and comparing the key molecular orbital (MO) transitions contributing to ECD Cotton effects in the 250-325 nm range.

Excited state transitions in this range were studied for the 10 most energetically favorable conformers of compound 2. It was found that each conformer exhibited exactly three electronic transitions at around 260, 277, and 295 nm, respectively. The 295 nm transitions were dominated by HOMO \rightarrow LUMO transition displaying solely $\pi \rightarrow \pi^*$ character, while the transitions near 277 nm showed exclusively $\sigma \rightarrow \pi^*$ character. The 260 nm transitions were also dominated by $\pi \rightarrow \pi^*$ character; however, two conformers showed some strong charge transfer contributions to this excited state as well. Examples of these characteristic MO transitions are shown in Figures 2, 3, and 4. By similarly analyzing electronic transitions for the remaining compounds, we hope to shed light on the common Cotton effect in each of the experimental ECD spectra.

■ RESULTS AND DISCUSSION

The general approach for utilizing theory to elucidate absolute configurations is straightforward (illustrated in Figure 5). Starting with an unresolved structure, stereogenic centers of the compound are identified, and initial structures are generated for all enantiomerically unique stereoisomers. It is only necessary to explore half of the total possible stereoisomers, because enantiomers will exhibit equal and opposite chiroptical properties. For a given stereoisomer, any stable ring

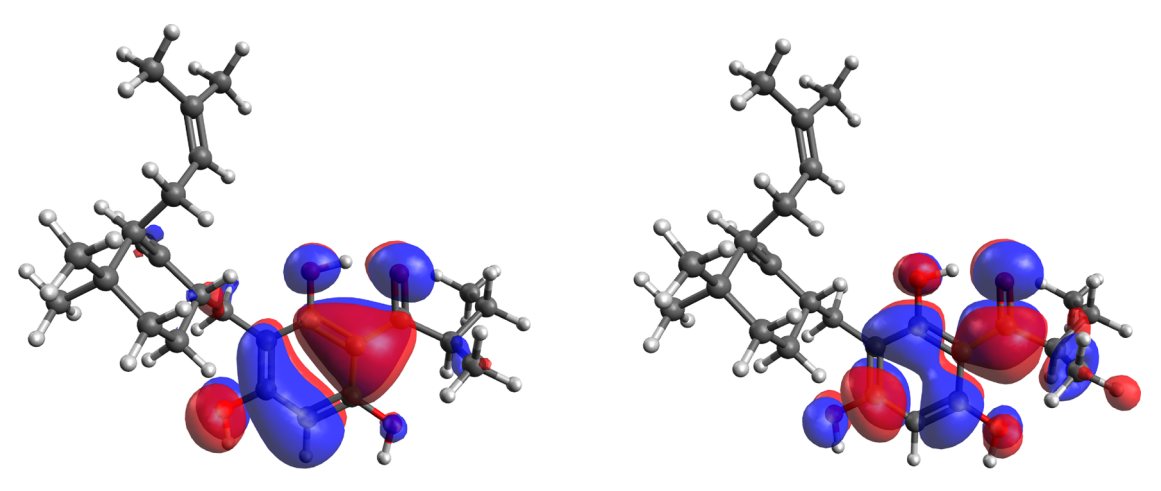


Figure 2. HOMO-2 \rightarrow LUMO ($\pi \rightarrow \pi^*$) MO transition for a conformer of 2.

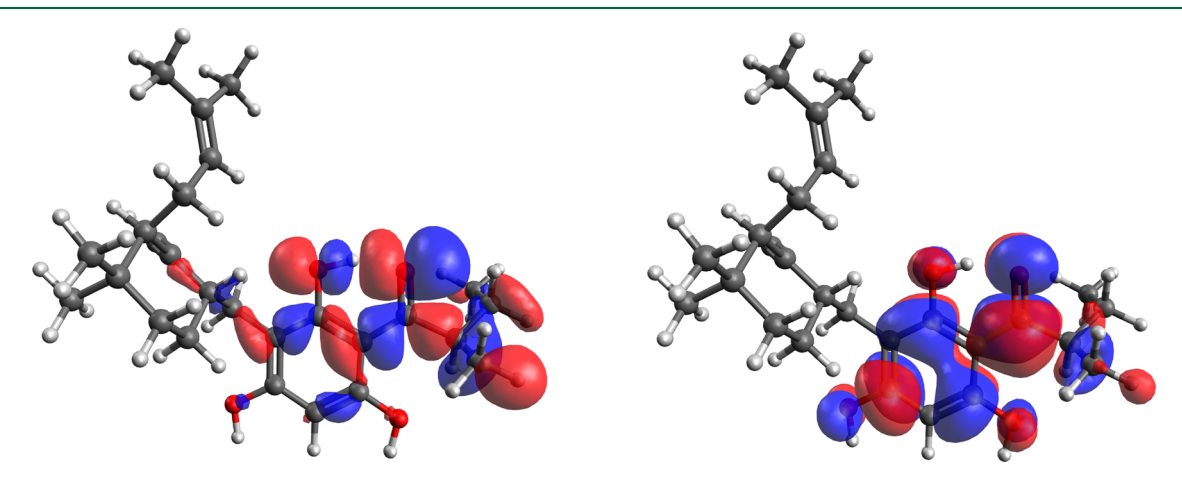


Figure 3. HOMO-4 \rightarrow LUMO ($\sigma \rightarrow \pi^*$) MO transition for a conformer of 2.

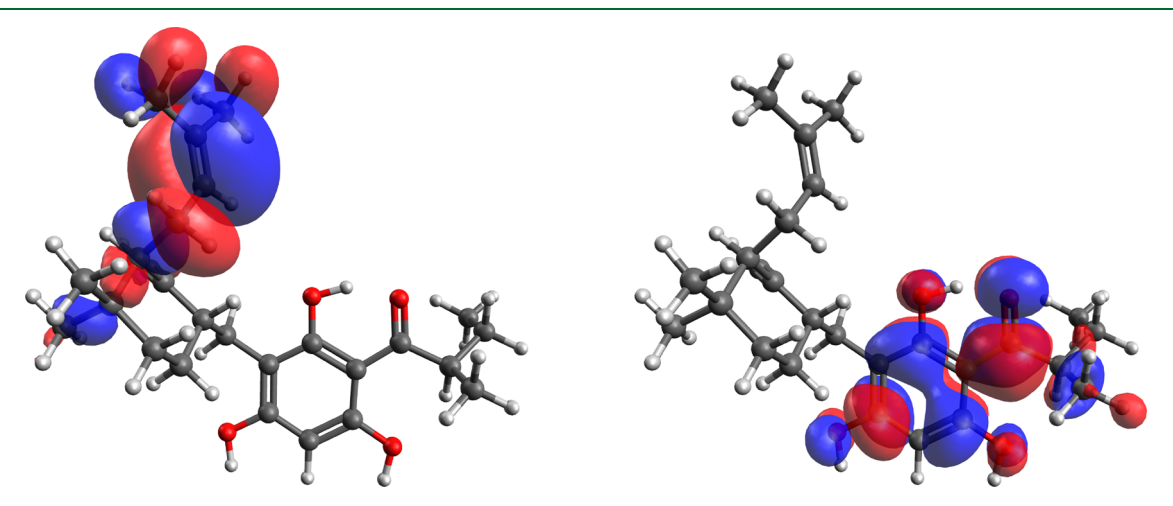


Figure 4. HOMO-1 \rightarrow LUMO (charge transfer) MO transition for a conformer of 2.

conformations are then determined using chemical knowledge or proposed stable conformations in the literature. Further side chain conformational searches for each ring conformer can be accomplished through a variety of approaches (molecular dynamics, Monte Carlo search algorithms, systematic rotation of torsional angles, among others). Owing to the highly flexible nature of many compounds of interest, this process is typically carried out at a molecular mechanics or semiempirical level in order to quickly ensure the consideration of all diverse low-

energy conformers. Initial conformations should adequately span the conformational space while acting as starting structures for more accurate energy minimizations. Each of these individual conformer geometries is then further optimized at a higher level of theory, typically using quantum chemical methods such as density functional theory (DFT) or wave function-based methods. Afterward, a relative absolute energy threshold is employed in order to eliminate duplicate conformers that relax to the same minimum on the potential

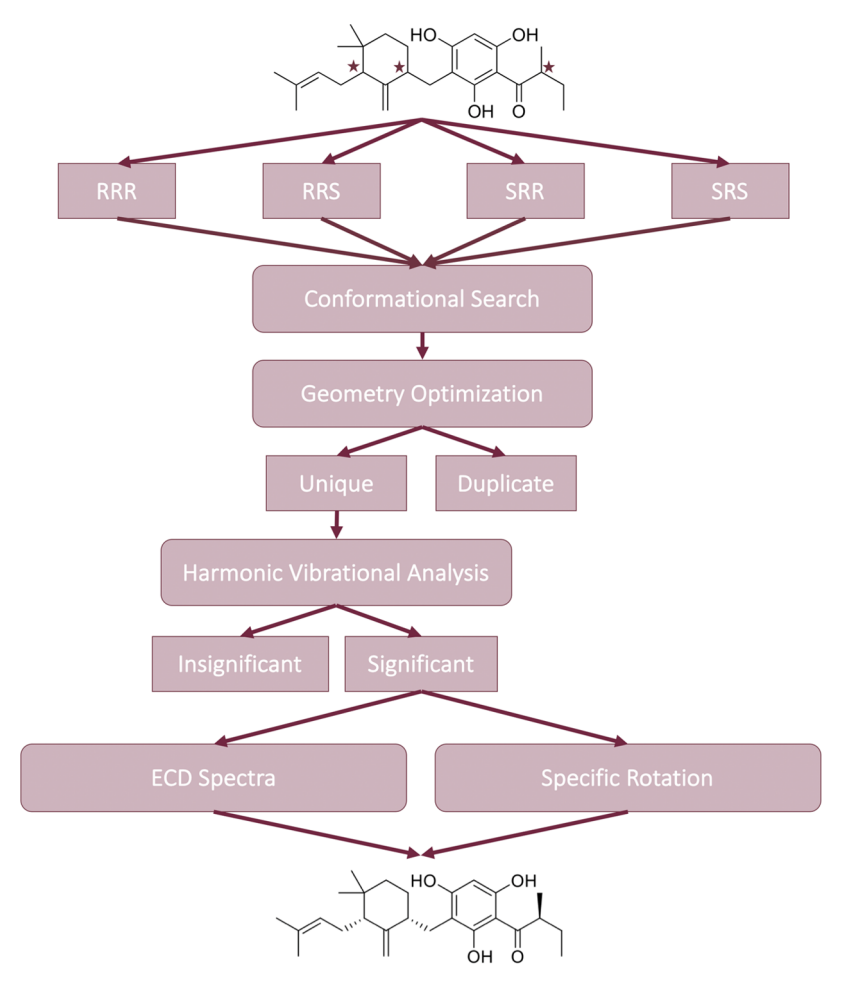


Figure 5. Stereochemical assignment flowchart.

energy surface. Harmonic vibrational analyses are then conducted for each unique geometry to confirm that the conformer lies at a true minimum while simultaneously computing a temperature-dependent Boltzmann population for each individual conformer. At this point, screening criteria are applied to determine which conformations are significantly populated at relevant temperatures. It is these unique and energetically favorable conformers that are finally subjected to the more computationally intensive ECD and specific rotation simulations, in which time-dependent density functional theory (TDDFT) is regularly employed.

Based on biosynthetic reasoning, the working hypothesis is that phloroglucinols 1–8 from *G. dauphinensis* would display the same absolute configurations at the 2-methylbutanoyl side chain. Similarly, it is expected that compounds 1 and 2 will have the same assignment at their additional shared C-4′ stereocenter. However, exceptions to this general rule are well-documented, ²⁹ and it is therefore still necessary to verify these assumptions for each of the remaining compounds by direct comparison of the computational results for all possible stereoisomers to their experimental counterparts. In order to accomplish this task, the general workflow outlined above was employed (specific computational details are described later in the Experimental Section). Herein, we report our findings for phloroglucinols 1 and 3–8 (Table 1).

Compound 1. In the case of compound 1, a tentative assignment of the configurations at C-4' and C-2" based on analogous assignments of compound 2 was previously reported

as (S)-2-methyl-1-(2,4,6-trihydroxy-3- $\{[(S)$ -2,4,4-trimethyl-3-(3-methylbut-2-en-1-yl)cyclohex-1-en-1-yl]methyl}phenyl)butan-1-one.²⁷ In order to confirm this assignment, ECD spectra were calculated for its (R, R) and (R, S) stereoisomers according to the procedure outlined above (the shorthand stereochemical descriptors refer to C-4' and C-2", respectively). The only calculated ECD spectrum that exhibited the same positive and negative Cotton effects as the experimental spectrum, albeit at slightly shorter wavelengths, was that of the (S, S) stereoisomer of 1 (Figure 6). As an additional comparison, specific rotations for both stereoisomers were calculated and compared to experimental values. Again, the calculated value of -86.0° dm⁻¹ (g/mL)⁻¹ for the (S, S) stereoisomer gave the best agreement in both sign and magnitude with the experimental value of -29.0° dm⁻¹ (g/ mL)⁻¹. On the basis of these data, the previously assigned structure of 1 is confirmed.

Electronic excited states and their associated MO transitions were also analyzed for the 10 most energetically favorable conformers of compound 1. Similar to compound 2, each conformer displayed three excited states each near 263, 283, and 297 nm. The excited states at 263 and 297 nm were comprised of purely $\pi \to \pi^*$ MO transitions as well as MO transitions with mixed $\pi \to \pi^*$ and charge transfer character. Additionally, excited states near both of these wavelengths contained significant contributions of HOMO \to LUMO transitions. Excitations near 283 nm were predominantly associated with pure $\sigma \to \pi^*$ MO transitions; however, about

Table 1. Absolute Configurations and Number of Conformers for Compounds 1 and 3-8

Cmpd	Structure	Number of Conformers		
		Total	Unique	Significant
1	4"" HO 1 OH 5" 2" OH O 4"	2459	656	161
3	8' 10' OH	7024	1531	390
4	HO OH OH OH OH	5525	961	262
5	OH HO OH (S) (R)	2180	854	246
6	8' HO 31 OH O (S)	1326	429	189
7	11 5	68	48	13
8	OH 4 (R) (S) 9 9 6" Ba (S) 6"	311	186	71

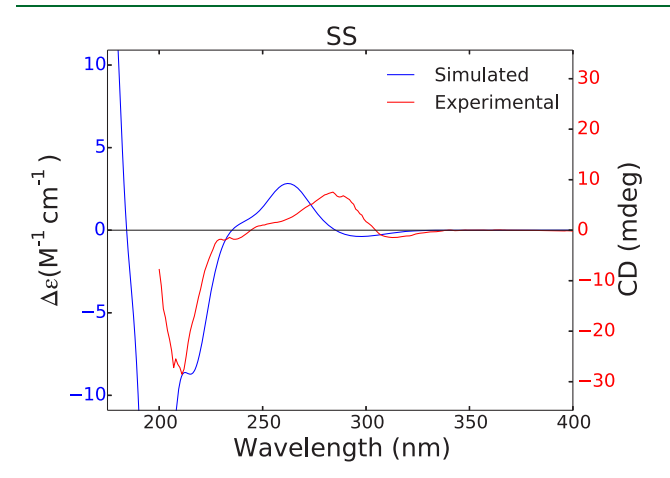


Figure 6. ECD spectrum of compound 1.

half of the conformers showed some mixed $\pi \to \pi^*$ and charge transfer character as well. With such similar types of MO

transitions defining the region near the positive Cotton effect, it is no surprise that the computed data confirmed an (S) assignment at the 2-methylbutanoyl side chain, identical to what was seen in compound 2.

Compound 3. In a similar manner, the absolute configuration of compound 3 was also determined by comparison of experimental and calculated ECD spectra and specific rotations. As before, the (2''S) configuration was tentatively assigned on the basis of the earlier assignment for compound 2; however, the configuration at C-2' remained unresolved. Simulated ECD spectra were generated for the (R, R) and (R, S) diastereomers (the shorthand stereochemical descriptors refer to the C-2' and C-2'', respectively), yet only the ECD spectrum of the (R, S) diastereomer featured corresponding maxima and minima at similar wavelengths to the experimental spectrum, shown in Figure 7. Moreover, the specific rotation for the (R, S) stereoisomer of 3 was calculated to be -4.6° dm⁻¹ $(g/mL)^{-1}$, which was by far the best agreement with the experimentally measured value of -3.3°

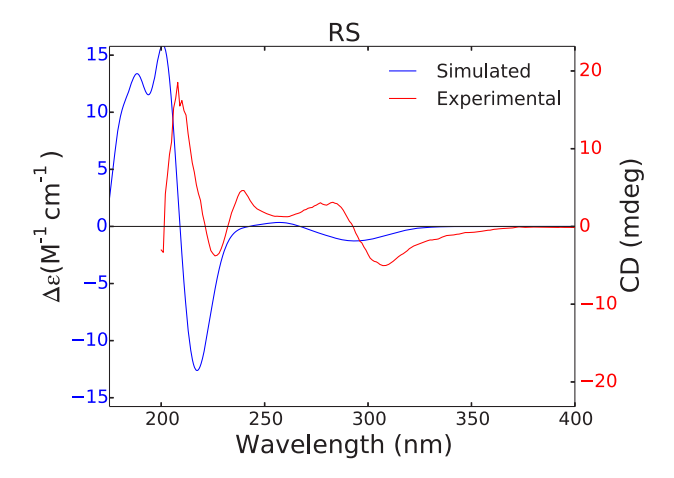


Figure 7. ECD spectrum of compound 3.

dm⁻¹ (g/mL)⁻¹, though comparison between theory and experiment for small-magnitude rotations such as these can be uncertain.³⁰ Therefore, compound 3 was identified as (2'R,2''S)-4-[2'-(3-methylbut-3-enyl)-3',7'-dimethylocta-3',6'-dienyl]-2-(2-methylbutanoyl)phloroglucinol.

The 10 conformers with the highest Boltzmann populations for compound 3 were also studied for the character of their electronic excited states. Within the 250–325 nm range, each conformer exhibited three electronic excitations at almost identical wavelengths as were seen in compound 1, viz. 263, 282, and 297 nm. Moreover, the transitions that characterize these excitations parallel those of compound 1 in that excitations near 263 and 297 nm were comprised of HOMO \rightarrow LUMO transitions that involved $\pi \rightarrow \pi^*$ and charge transfer character in addition to other MO transitions that were entirely $\pi \rightarrow \pi^*$ in character. Excitations near 282 nm for 3 were comprised of $\sigma \rightarrow \pi^*$ transitions alone. These nearly identical characteristics further support the expectation that compounds 1, 2, and 3 would have the same C-2" absolute configuration.

Compound 4. The ECD spectra and specific rotation of compound 4 were calculated for the (R, R) and (R, S) stereoisomers (the shorthand stereochemical descriptors refer to C-2' and C-2", respectively) in order to affirm the presumed (2"S) configuration and determine the absolute configuration at C-2'. Upon comparison to the experimental spectrum, (R, S) was the only reasonable match, shown in Figure 8. The calculated specific rotation for (R, S) also had the best agreement with experiment (+25.3 and +5.3, respectively). These data support the previous configurational assumptions, and compound 4 was thus identified as (2'R, 2"S)4-[3', 7'-dimethyl-2'-(3-methylbut-2-en-1-yl)octa-3', 6'-dien-1'-yl]-2-(2-methylbutanoyl)phloroglucinol.

An analogous investigation of the most populated conformers of compound 4 revealed exceedingly similar excited state character with respect to those previously discussed. Specifically, three excited states were present for each conformer in the specified region at equivalent wavelength values as were found in compound 3. The MO transitions around 282 nm resembled the same pure $\sigma \to \pi^*$ nature. The only noticeable difference was that transitions near 263 and 297 nm did not show exclusive $\pi \to \pi^*$ character; rather, each of these transitions were comprised of both $\pi \to \pi^*$ and charge transfer character, albeit at varying levels. Excited states near 297 nm were dominated by HOMO \to LUMO transitions,

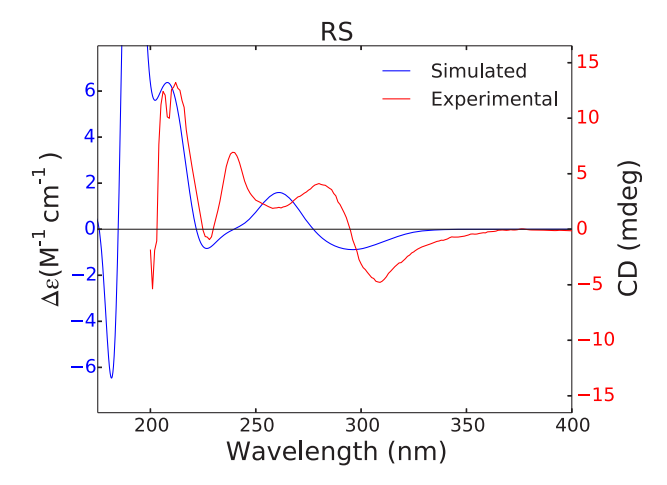


Figure 8. ECD spectrum of compound 4.

while excited states near 263 nm were comprised mostly of HOMO-2 \rightarrow LUMO and HOMO-3 \rightarrow LUMO transitions.

Compound 5. For compound 5, there was no experimentally measured ECD spectrum, and therefore, a comparison to experiment could only be carried out for specific rotation values. As such, specific rotations were calculated for both the (R, R) and (R, S) diastereomers (the shorthand stereochemical descriptors refer to C-2' and C-2", respectively) and subsequently compared to the experimental specific rotation of -13.9° dm⁻¹ (g/mL)⁻¹. Upon comparison, the calculated specific rotation for the (S, R) stereoisomer of -19.0° dm⁻¹ (g/mL)⁻¹ gave the best agreement with respect to sign and magnitude. Based on this sole comparison, we tentatively assign compound 5 as (2'S,2"R)4-[3',7'-dimethyl-2'-(3- hydroxy-3-methylbutyl)octa-3',6'-dien-1'-yl]-2-(2"methylbutanoyl)phloroglucinol. It should be noted that this is the first instance where the previous tentative assignment at C-2" is called into question. The calculated ECD spectrum of the (S, R) diastereomer is also reported in Figure 9.

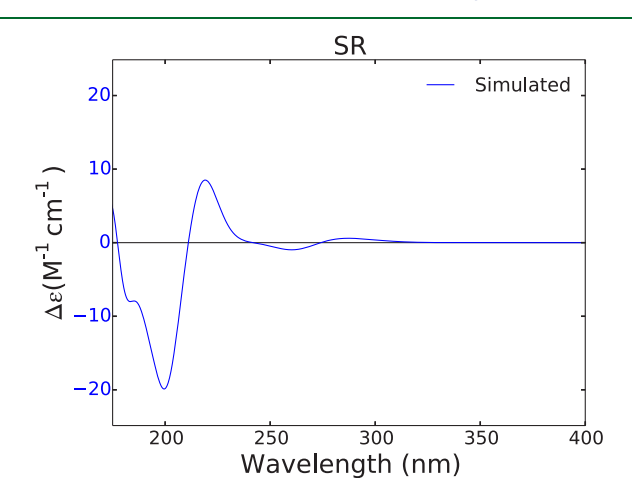


Figure 9. Simulated ECD spectrum of compound 5.

As a consequence of having no experimental ECD spectrum, there was also no experimental Cotton effect to examine. However, the calculated spectrum does in fact exhibit an analogous negative Cotton effect where positive Cotton effects have been seen in the other simulated and experimental spectra. As such, it was worth conducting a similar MO analysis of the transitions that contributed most significantly to the

observed Cotton effect. The analysis revealed that each of the 10 lowest-energy conformers possessed three excited states of interest around 263, 282, and 298 nm. As seen previously, the excited state transitions near 298 nm were dominated by HOMO \rightarrow LUMO transitions of $\pi \rightarrow \pi^*$ character; however, transitions involving some additional charge transfer contributions were seen in most conformers as well. As observed in almost every other compound, the MO transitions that made up the excited states near 282 nm were exclusively $\sigma \rightarrow \pi^*$ in character. Lastly, excitations near 263 nm originated from pure $\pi \rightarrow \pi^*$ type transitions as well as mixed transitions that were more heavily dominated by charge transfer character with additional $\pi \rightarrow \pi^*$ character.

Although compound 5 was assigned as the (S, R) stereoisomer, it is worth mentioning that its (R, S) enantiomer shares the same excited states and characteristic MO transitions. Additionally, the calculated ECD spectrum for the (R, S) stereoisomer exhibits a similar positive Cotton effect to those seen in each of the other phloroglucinols from G. dauphinensis, as opposed to the uncharacteristic negative Cotton effect seen in the spectrum of the (S, R) isomer above (Figure 9). It is also worth noting that the ECD spectrum for the (S, R) stereoisomer exhibits inverted features, especially at low wavelengths, when compared to all other compounds. While this is not enough evidence to change our assignment, it further weakens the (S, R) assignment, which we hope will spur additional experimental spectroscopic analysis of this compounds.

Compound 6. As above, in order to determine the absolute configuration of compound **6**, ECD and specific rotations were calculated for the (R, R) and (R, S) diastereomers (the shorthand stereochemical descriptors refer to C-3' and C-2", respectively). When compared to the experimental data, it was determined that the best fit was for the (R, S) stereoisomer. While the agreement is not perfect, the simulated spectrum for the (R, S) diastereomer (Figure 10) was the only one to exhibit

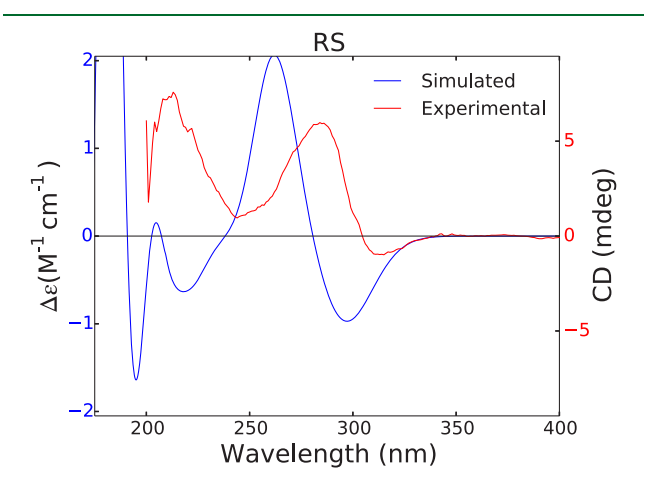


Figure 10. ECD spectrum of compound 6.

the same qualitative features especially at the longer wavelength regions. Additionally, the calculated specific rotation for the (R, S) stereoisomer had a strong match with the experimental value (19.4 and 18.2° dm⁻¹ (g/mL)⁻¹, respectively). As a result, the identification of **6** was confirmed as (3'R, 2''S)4-(3'-hydroxy-3',7'-dimethyloct-6'-en-1'-yl)-2-(2-methylbutanoyl)phloroglucinol.

Relevant excited state transitions for the 10 most populated conformers of compound 6 occurred around 263, 282, and 297 nm, involving nearly identical MO transitions for every conformer. Excitations near 263 and 297 nm were characterized by three types of transitions: pure $\pi \to \pi^*$ (HOMO-2 \rightarrow LUMO), predominantly charge transfer with some $\pi \rightarrow \pi^*$ character (HOMO-1 \rightarrow LUMO), and majority $\pi \rightarrow \pi^*$ character with some charge transfer (HOMO \rightarrow LUMO). On the other hand, HOMO-3 → LUMO transitions predominantly defined the 282 nm excited state, which was shown to be entirely $\sigma \to \pi^*$ in character. These transitions were typical of what was seen in compound 2 as well as the other phloroglucinols, further supporting the common Cotton effect exhibited in each experimental spectra. We also note that, as pointed out by a reviewer, changes in configuration around the C-3' stereocenter of 6 appear to result in significant changes to the long-wavelength ECD spectroscopic features (cf. Figures S20 and S21, Supporting Information) even though this carbon is distant from the presumed chromophores. However, our analysis of the MOs involved in two of the key transitions between 260 and 300 nm reveal participation by the nonbonded orbitals on the oxygen atom of the 3'-hydroxy group.

Compound 7. Simulated ECD spectra and specific rotations were generated for all enantiomerically unique stereoisomers of compound 7. However, due to similarities in the experimental ¹H and ¹³C NMR data of the known phloroglucinol derivative, hyperjovinol B,31 relative configurations at C-8a and C-10a were previously established for compound 7 and it was identified as $1-[(8aR^*,10aR^*)-1,3$ dihydroxy-8,8,10a-trimethyl-5,6,7,8a,9,10a-hexahydro-1Hxanthen-2-yl]-2-methylbutan-1-one.²⁷ Accordingly, ECD spectra comparisons for stereoisomers that exhibit this relative configuration are shown in Figure 11. The (R, R, R) and (R, R, R)S) diastereomers appear to match the experimental ECD spectrum fairly well with the most notable difference being the lack of a negative Cotton effect in the simulated spectrum for the (R, R, S) isomer above 300 nm (the shorthand stereochemical descriptors refer to C-8a, C-10a, and C-2', respectively). Moreover, the calculated specific rotation for (R, $(g/mL)^{-1}$, had better agreement than the calculated rotation for (R, R, S), 205.5° dm⁻¹ $(g/mL)^{-1}$, when compared to the experimental value of 11.0° dm⁻¹ (g/mL)⁻¹, though the difference in magnitude of the rotation weakens the assignment. Thus, based on these data, compound 7 was identified as (8aR,10aR,2'R)1-[1,3-dihydroxy-8,8,10a-trimethyl-5,6,7,8a,9,10a-hexahydro-1*H*-xanthen-2-yl]-2-methylbutan-1-one. Again, it is worth noting that this assignment contradicts the presumed (S) configuration at C-2" based on the assignment of an identical stereocenter of the representative compound 2.

The limited conformational flexibility of compound 7 resulted in only four conformations of the (R, R, R) stereoisomer with significant Boltzmann populations. Each of these conformers contained three excited states of interest at 268, 281, and 296 nm, respectively. It was found that the 268 and 296 nm excitations consisted of the exact same two MO transitions: HOMO-1 \rightarrow LUMO and HOMO \rightarrow LUMO, both of which were entirely $\pi \rightarrow \pi^*$ in nature. Additionally, the remaining excitation at 281 nm was characterized by transitions involving strictly $\sigma \rightarrow \pi^*$ character. All of these transitions were highly similar to what was seen in the representative compound 2; however, their final assignments

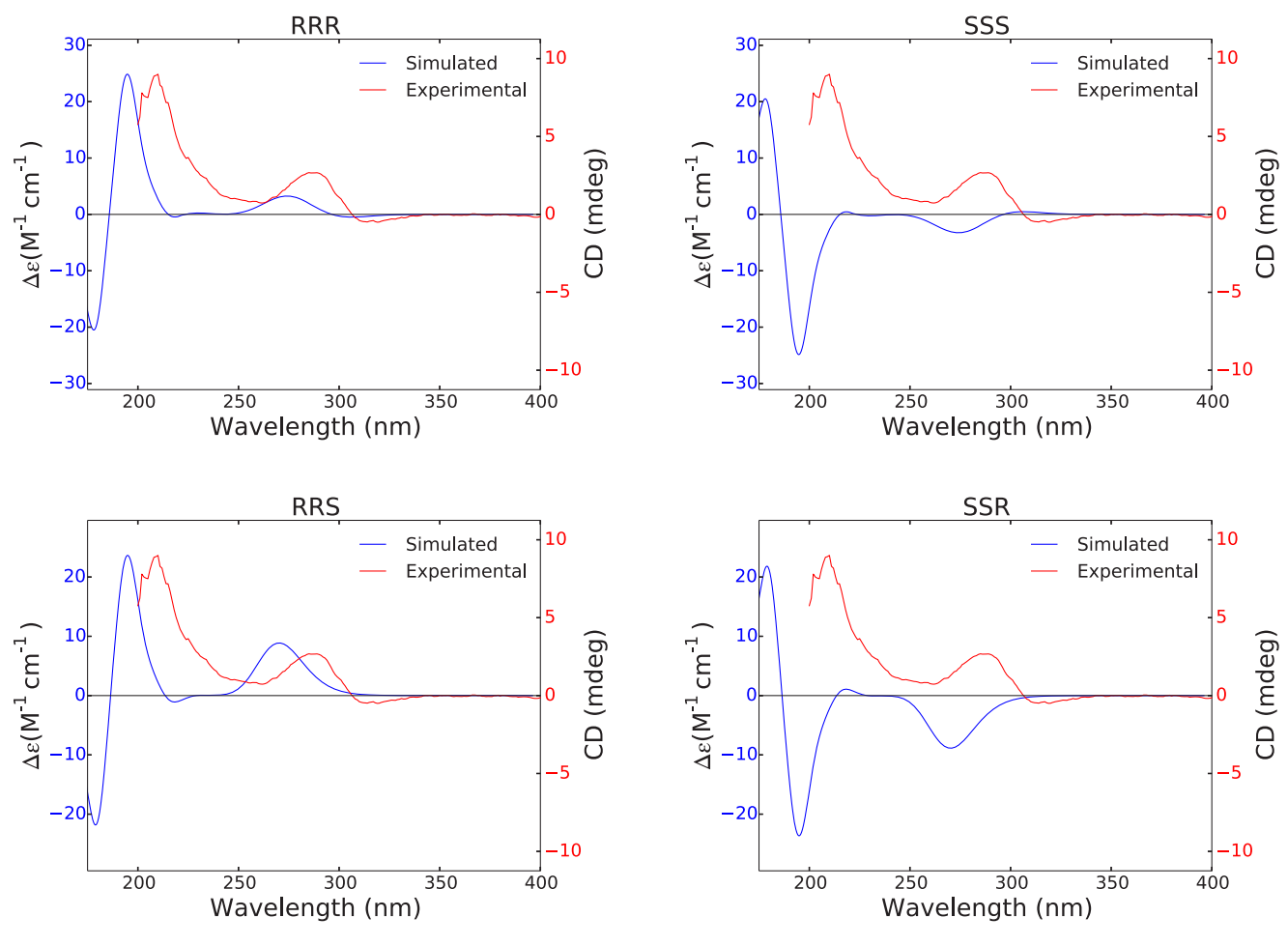


Figure 11. ECD spectra of four diastereomers of compound 7.

differ at their shared stereocenter on the 2-methylbutanoyl side chain.

Compound 8. Compound 8 was found to be a known phloroglucinol that had been previously identified as $1-[(2R^*,$ $3S^*$)-3,5,7-trihydroxy-2-methyl-2-(4-methyl-pent-3-enyl)chroman-8-yl]-2-methylbutan-1-one.³² Although ECD spectra and specific rotations were calculated for all possible diastereomers, only results for stereoisomers with the specified relative configuration are shown in Figure 12. From these results, the only two reasonable simulated ECD spectra are for the (S, R, S) and (S, R, R) stereoisomers (the shorthand stereochemical descriptors refer to C-2, C-3 and C-2', respectively); however, neither of these shows a particular strong match with the experimental spectrum. Unfortunately, subsequent comparison of the simulated specific rotations gave little further insight into the elucidation of the structure of 8 as calculated values for both the (S, R, S) and (S, R, R) diastereomers (83.2 and 67.1° dm⁻¹ (g/mL)⁻¹, respectively) gave agreeable comparisons to the experimental value of 60° $dm^{-1} (g/mL)^{-1}$. Nevertheless, it is likely based on biosynthetic reasoning that C-2' possesses an (S) configuration like a majority of the phloroglucinols isolated from G. dauphinensis. Thus, the identity for compound 8 is tentatively confirmed as (2S,3R,2'S)1-[3,5,7-trihydroxy-2-methyl-2-(4-methyl-pent-3enyl)chroman-8-yl]-2-methylbutan-1-one.

None of the simulated spectra in Figure 12 portrayed the Cotton effect that was present in the experimental spectrum. Nonetheless, it is worth examining the orbital transitions that

make up the most prominent features in the 250–325 nm range. As such, the 10 conformers with the highest Boltzmann populations were analyzed for their excited state character. Each conformer exhibited exactly three electronic excited states in the specified region around 266, 283, and 299 nm. The MO transitions associated with the 299 nm transition were purely $\pi \to \pi^*$ in character, whereas the 283 nm excitations were characterized by $\sigma \to \pi^*$ transitions exclusively. Excited states near 266 nm showed a mix of $\pi \to \pi^*$ and charge transfer character. The excited states near 299 nm were almost exclusively defined by HOMO \to LUMO transitions, while all three excited states that were mentioned were dominated by transitions into the LUMO. Each of these types of transitions was typical when compared to those observed in the other compounds.

CONCLUSIONS

Seven new phloroglucinols 1–7 as well as the known phloroglucinol (8) were recently isolated from a native plant species of Madagascar, *G. dauphinensis*. The isolated compounds were subsequently tested and were reported to have good to moderate anticancer and antiproliferative activities. Experimental ECD spectra and specific rotations were previously reported;²⁷ however, due to the conformational flexibility of the molecules, only 2 was previously studied computationally in order to determine its absolute configuration. While tentative assignments were given to 1 and 3–8 based on biological reasoning, definitive absolute configurations.

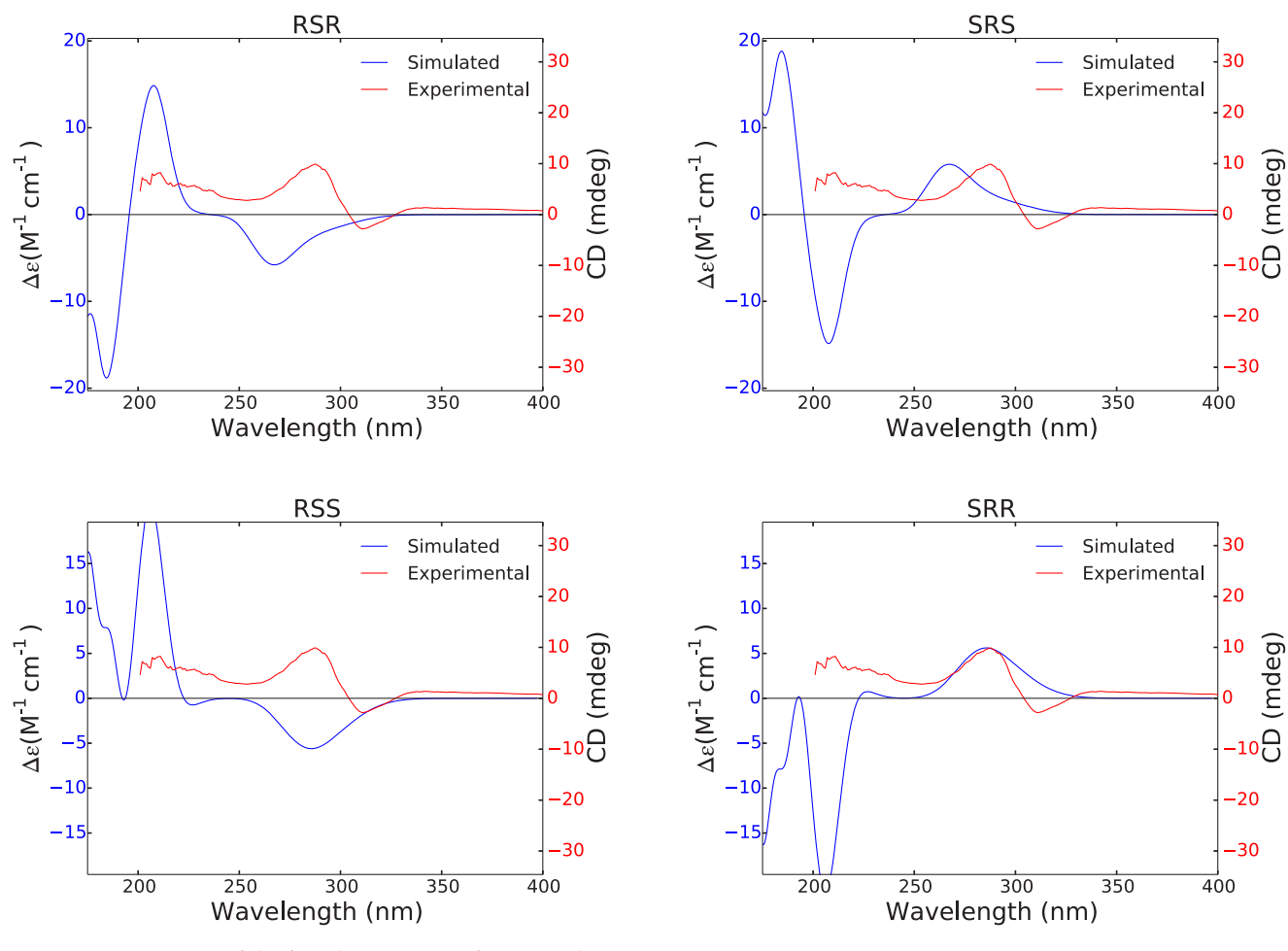


Figure 12. ECD spectra of the four diastereomers of compound 8.

rations based on the direct comparison of experimental and simulated ECD spectra and specific rotations remained to be assigned. As such, we report the first computational results for compounds 1 and 3–8 as well as their absolute configurations.

The degree of confidence in our assignments relies heavily on the comparison of the simulated and experimental data. As the conformational space and number of stereogenic centers increase, it can become less clear which stereoisomer has the best match. This is evident in the example of compound 2, where a definitive assignment could not be made based on the ECD and specific rotation data alone, because two separate stereoisomers showed data that agreed reasonably well with experiment. As such, additional NOESY data were recorded and compared against key internuclear distances in order to arrive at a relative configuration first.²⁷ In the case of compounds 1 and 3–8, NOESY data were not available, and thus, assignment had to be made based solely on the ECD and specific rotations data at hand. As such, various degrees of certainty are reported with each assignment.

Compounds 1, 3, 4, and 6 had the most unequivocal assignments by far. In each case, comparison to experiment resulted in a single stereoisomer that exhibited reasonable computational results, allowing for a straightforward assignment. The assignment of compound 5 proved to be more difficult due to the absence of an experimental ECD spectrum. In that case, an assignment was made entirely based on which stereoisomer exhibited the most similar specific rotation when compared to the experiment. However, this comparison can

become less reliable on its own when dealing with specific rotation values that are small in magnitude, as was the case with 5. As such, we are less confident in the assignment for compound 5. As for compounds 7 and 8, we were operating under the constraint of a previously determined relative configuration. None of the stereoisomers with the appropriate relative configurations showed particularly strong comparison across both experiments, and thus, we report our assignments for these compounds with only a moderate level of confidence.

As a further analysis with respect to the positive Cotton effect which was depicted in every experimental ECD spectrum available, excited states in the 250-325 nm region were explored for the most significant conformers of each compound. It was found that every compound exhibited three excited electronic states at very similar wavelengths, and there were few noticeable differences in the MO transitions which made up these specified excitations. In general, the highest energy excited state in this region was dominated by π $\rightarrow \pi^*$ character with some compounds showing charge transfer character as well. The lowest energy excited state for each compound was typically made up of transitions involving both $\pi \to \pi^*$ and charge transfer character. Lastly, the middle excited state almost always showed exclusive $\sigma \to \pi^*$ character. These results were unsurprising as we expected to see similar transitions defining the positive Cotton effect which was present in every experimental ECD spectrum.

It is worth noting that compounds 1-8 appear to belong to two different stereochemical families, namely, 1-4, 6, and 8

having the (*S*) configuration at the 2-methylbutanoyl side chain, whereas **5** and 7 exhibit the (*R*) configuration at the analogous stereocenter. These discrepancies may be attributed to less reliable assignments; however, it is also possible that compounds **5** and 7 belong to the opposite stereochemical series as the rest of the phloroglucinols from *G. dauphinensis*. Nevertheless, violation of this general rule is not unprecedented, and similar instances have been well-documented.²⁹

EXPERIMENTAL SECTION

Computational Details. The key components for the prediction of ECD spectra involve excitation energies for a given transition $0 \rightarrow n$, ω_{n0} , and their associated rotatory strengths, R_{n0} , given as the dot product of the transition electric- and magnetic-dipole moments:³³

$$R_{n0} = \operatorname{Im}\{\langle 0|\boldsymbol{\mu}|n\rangle \cdot \langle n|\boldsymbol{m}|0\rangle\} \tag{1}$$

where $|0\rangle$ denotes the ground-state wave function, $|n\rangle$ denotes an electronically excited-state wave function, $\mu = \sum_i q_i r_i$ is the electric-dipole operator, $m = \sum_i \frac{q_i}{2m_i} r_i \times p_i$ is the magnetic dipole operator, and "Im" indicates that only the imaginary part of the expression is retained.

In the case of specific rotation, the central quantum mechanical quantity is the electric-dipole magnetic-dipole polarizability tensor, first derived by Rosenfeld in 1929³⁴

$$\beta(\omega) = -\frac{2\omega}{\hbar} \text{Im} \sum_{n \neq 0} \frac{\langle 0|\mu|n\rangle\langle n|m|0\rangle}{\omega_{n0}^2 - \omega^2}$$
(2)

where ω is the frequency of the incident radiation field and the summation runs over all electronically excited states. The specific rotation (in degrees (deg) dm⁻¹ (g/mL)⁻¹), $[\alpha]_{\omega}$, is directly related to the trace of β according to³³

$$\left[\alpha\right]_{\omega} = \frac{(72.0 \times 10^6)\hbar^2 N_{A}\omega}{c^2 m_e^2 M} \times \left[\frac{1}{3} \text{Tr}(\beta)\right] \tag{3}$$

where β and ω are given in atomic units, N_A is Avogadro's number, c is the speed of light (m/s), m_e is the electron rest mass (kg), and M is the molecular mass (amu). The prefactor in eq 3 accounts for averaging over all molecular orientations. Finally, results for individual conformers are combined according to their Boltzmann populations to produce weighted average spectra and specific rotations for each stereoisomer that can be directly compared to experimental data. We note that, while vibrational effects on specific rotations, including zero-point vibrational motion, have been found to be significant in some cases, $^{35-40}$ the computational demands of including such factors for molecules of this size and for such large numbers of conformers precludes their consideration in the present study.

Side chain conformational searches for each ring conformer were generated by systematically rotating dihedral angles along all rotatable bonds in the molecule using the Open Babel software⁴¹ in conjunction with the MMFF94 force field⁴² and the Confab systematic rotor conformer generator.⁴³ An energy cutoff of 10 kcal/mol was employed such that only side chain conformers with a relative energy less than that of the cutoff were kept. In agreement with previous studies of structurally similar compounds, geometries were optimized at the DFT/B3LYP/6-31G* level of theory 44-47 within a MeOH solvent simulated using the polarizable continuum model (PCM).⁴⁸ Harmonic vibrational frequencies were also computed at the same level of theory to ensure that no imaginary values were present, thus confirming that all of the structures were minima on their respective potential energy surfaces. Thermal Gibbs free energies were obtained using partition functions computed within the harmonic oscillator/rigid rotor approximations, ^{49,50} permitting the calculation of room-temperature equilibrium Boltzmann populations. Conformers with the most significant Boltzmann populations were kept until >90% of the total population was accounted for. Excitation energies and rotatory strengths for each transition (in the velocity

representation) were calculated for the first 40 electronic excited states at the TDDFT/CAM-B3LYP/aug-cc-pVDZ level of theory, 51-53 again including the PCM description of the MeOH solvent. Once more, the functional and basis set were found to be appropriate when compared to previous studies of this nature. 54-56 The ECD spectra were simulated by overlapping Gaussian functions for each transition according to 57

$$\Delta \varepsilon(\tilde{\nu}) = \frac{1}{(2.296 \times 10^{-39})\pi\sigma} \sum_{a} \tilde{\nu}_{n0} R_{n0} \exp\left[-\left\{\frac{(\tilde{\nu} - \tilde{\nu}_{n0})}{\sigma}\right\}^{2}\right]$$
(4)

where σ is defined as half the bandwidth at 1/e peak height and $\tilde{\nu}_{n0}$ is equivalent to ω_{n0} but in units of wavenumbers. The σ value is an empirical parameter, and we chose a value of 0.50 eV in agreement with the resolution of the experimental ECD bandwidths. The vertical axes of ECD spectra were scaled in order to normalize the most prominent peak heights between the simulated and experimental values. The horizontal axes limits were chosen such that features of the predicted spectra were shown beyond the limits of the experimental apparatus at 200 nm. No scaling or shifts on the energy/wavelength scale were applied, as the CAM-B3LYP functional has been shown to be less prone to consistent underestimation of excitation energies. Specific rotations were calculated at the TDDFT/ CAM-B3LYP/aug-cc-pVDZ level of theory utilizing a PCM solvent as well. Weighted average ECD spectra and specific rotations for all possible stereoisomers of compounds 1 and 3-8 are included in the Supporting Information. Lastly, single point energy calculations at the DFT/CAM-B3LYP/aug-cc-pVDZ level of theory were carried out on the optimized geometries of the 10 most significant conformers for each compound such that the key MO transitions contributing to their ECD spectra could be visualized. An isosurface value of 0.02 was used for the rendering of all molecular orbitals. Representative MO transitions for each compound are also available in the Supporting Information. All calculations were performed using the Gaussian 09 electronic structure package.

ASSOCIATED CONTENT

Supporting Information

The Supporting Information is available free of charge at https://pubs.acs.org/doi/10.1021/acs.jnatprod.0c01208.

Comparison of experimental and calculated ECD spectra for all possible stereoiosmers of compounds 1 and 3–8, comparison of experimental and calculated specific rotations for all possible stereoiosmers of compounds 1 and 3–8, and characterisitic MO transitions for compounds 1 and 3–8 (PDF)

AUTHOR INFORMATION

Corresponding Author

T. Daniel Crawford – Department of Chemistry, Virginia Tech, Blacksburg, Virginia 24061, United States; Molecular Sciences Software Institute, Blacksburg, Virginia 24060, United States; orcid.org/0000-0002-7961-7016; Phone: +1 (540)231 7760; Email: crawdad@vt.edu

Authors

Kirk C. Pearce – Department of Chemistry, Virginia Tech, Blacksburg, Virginia 24061, United States; orcid.org/ 0000-0001-8033-6310

Rolly G. Fuentes — Department of Chemistry and Virginia Tech Center for Drug Discovery, Virginia Tech, Blacksburg, Virginia 24061, United States; Division of Natural Sciences and Mathematics, University of the Philippines Visayas Tacloban College, 6500 Tacloban City, Philippines

- Susana Calderon Department of Chemistry, Virginia Tech, Blacksburg, Virginia 24061, United States
- Rageshwari Marolikar Department of Chemistry, Virginia Tech, Blacksburg, Virginia 24061, United States
- David G. I. Kingston Department of Chemistry and Virginia Tech Center for Drug Discovery, Virginia Tech, Blacksburg, Virginia 24061, United States; orcid.org/0000-0001-8944-246X

Complete contact information is available at: https://pubs.acs.org/10.1021/acs.jnatprod.0c01208

Notes

The authors declare no competing financial interest.

ACKNOWLEDGMENTS

This project was supported by the U.S. National Science Foundation via Grant CHE-1900420. The authors acknowledge Advanced Research Computing at Virginia Tech for providing computational resources and technical support that have contributed to the results reported within this paper. K.C.P. acknowledges a graduate fellowship from the Virginia Tech Institute for Critical Technology and Applied Science (ICTAS). R.G.F. is grateful for a Postdoctoral Research Scholarship from the Science, Technology, Research, and Innovation Development (STRIDE) Program of USAID.

REFERENCES

- (1) Kingston, D. G. J. Nat. Prod. 2011, 74, 496-511.
- (2) In Biologically Active Natural Products: Pharmaceuticals; Cutler, S. J., Cutler, H. G., Eds.; CRC Press, 2000.
- (3) Newman, D. J.; Cragg, G. M. J. Nat. Prod. 2012, 75, 311-335.
- (4) Chen, Q.-F.; Liu, Z.-P.; Wang, F.-P. Mini-Rev. Med. Chem. 2011, 11, 1153-1164.
- (5) Le Marchand, L. Biomed. Pharmacother. 2002, 56, 296-301.
- (6) Nijveldt, R. J.; Van Nood, E.; Van Hoorn, D. E.; Boelens, P. G.; Van Norren, K.; Van Leeuwen, P. A. Am. J. Clin. Nutr. **2001**, 74, 418–425
- (7) Negi, J. S.; Bisht, V. K.; Singh, P.; Rawat, M. S. M.; Joshi, G. P. J. Appl. Chem. 2013, 2013, 1–9.
- (8) Pal Singh, I.; Bharate, S. B. Nat. Prod. Rep. 2006, 23, 558-591.
- (9) Flack, H. D.; Bernardinelli, G. Chirality 2008, 20, 681-690.
- (10) Polavarapu, P. L. Mol. Phys. 1997, 91, 551-554.
- (11) Polavarapu, P. L.; Chakraborty, D. K. J. Am. Chem. Soc. 1998, 120, 6160-6164.
- (12) Furche, F.; Ahlrichs, R.; Wachsmann, C.; Weber, E.; Sobanski, A.; Vögtle, F.; Grimme, S. J. Am. Chem. Soc. 2000, 122, 1717–1724.
- (13) Stephens, P. J.; Devlin, F. J.; Cheeseman, J. R.; Frisch, M. J. J. Phys. Chem. A **2001**, 105, 5356–5371.
- (14) Polavarapu, P. L. Chirality 2002, 14, 768-781.
- (15) Stephens, P. J.; Devlin, F. J.; Cheeseman, J. R.; Frisch, M. J.; Rosini, C. Org. Lett. **2002**, *4*, 4595–4598.
- (16) Diedrich, C.; Grimme, S. J. Phys. Chem. A 2003, 107, 2524–2539.
- (17) Pecul, M.; Ruud, K.; Helgaker, T. Chem. Phys. Lett. 2004, 388, 110–119.
- (18) Pecul, M.; Marchesan, D.; Ruud, K.; Coriani, S. J. Chem. Phys. 2005, 122, 024106.
- (19) Crawford, T. D. Theor. Chem. Acc. 2006, 115, 227-245.
- (20) Crawford, T. D. In Comprehensive Chiroptical Spectroscopy: Instrumentation, Methodologies, and Theoretical Simulations; Berova, N., Polavarapu, P. L., Nakanishi, K., Woody, R. W., Eds.; John Wiley & Sons, Inc., 2012; pp 675–697.
- (21) Li, X.-C.; Ferreira, D.; Ding, Y. Curr. Org. Chem. 2010, 14, 1678-1697.
- (22) Crawford, T. D.; Tam, M. C.; Abrams, M. L. J. Phys. Chem. A 2007, 111, 12057-68.

- (23) Nugroho, A. E.; Morita, H. J. Nat. Med. 2014, 68, 1-10.
- (24) Du, Y.; Pearce, K. C.; Dai, Y.; Krai, P.; Dalal, S.; Cassera, M. B.; Goetz, M.; Crawford, T. D.; Kingston, D. G. I. *J. Nat. Prod.* **2017**, *80* (5), 1639–1647.
- (25) Bringmann, G.; Bruhn, T.; Maksimenka, K.; Hemberger, Y. Eur. J. Org. Chem. **2009**, 2009, 2717–2727.
- (26) Giorgio, E.; Viglione, R. G.; Zanasi, R.; Rosini, C. *J. Am. Chem. Soc.* **2004**, *126*, 12968–12976.
- (27) Fuentes, R. G.; Pearce, K. C.; Du, Y.; Rakotondrafara, A.; Valenciano, A. L.; Cassera, M. B.; Rasamison, V. E.; Crawford, T. D.; Kingston, D. G. *J. Nat. Prod.* **2019**, *82*, 431–439.
- (28) Morton, B. R. A.; Stubbs, A. L. J. Chem. Soc. 1940, 1347-1359.
- (29) Finefield, J. M.; Sherman, D. H.; Kreitman, M.; Williams, R. M. Angew. Chem., Int. Ed. 2012, 51, 4802–4836.
- (30) Stephens, P. J.; McCann, D. M.; Cheeseman, J. R.; Frisch, M. J. Chirality 2005, 17, 52–64.
- (31) Athanasas, K.; Magiatis, P.; Fokialakis, N.; Skaltsounis, A. L.; Pratsinis, H.; Kletsas, D. J. Nat. Prod. 2004, 67, 973–977.
- (32) Schmidt, S.; Jürgenliemk, G.; Schmidt, T. J.; Skaltsa, H.; Heilmann, J. J. Nat. Prod. 2012, 75, 1697–1705.
- (33) Barron, L. Molecular Light Scattering and Optical Activity, 2nd ed.; Cambridge University Press: Cambridge, UK, 2004.
- (34) Rosenfeld, L. Eur. Phys. J. A 1929, 52, 161-174.
- (35) Ruud, K.; Taylor, P. R.; Åstrand, P.-O Chem. Phys. Lett. 2001, 337, 217-223.
- (36) Ruud, K.; Zanasi, R. Angew. Chem., Int. Ed. 2005, 44, 3594-3596
- (37) Crawford, T. D.; Tam, M. C.; Abrams, M. L. Mol. Phys. 2007, 105, 2607-2617.
- (38) Kongsted, J.; Ruud, K. Chem. Phys. Lett. 2008, 451, 226-232.
- (39) Pedersen, T. B.; Kongsted, J.; Crawford, T. D.; Ruud, K. J. Chem. Phys. 2009, 130, 034310.
- (40) Pedersen, T. B.; Kongsted, J.; Crawford, T. D. Chirality 2009, 21, S68-S75.
- (41) O'Boyle, N. M.; Banck, M.; James, C. A.; Morley, C.; Vandermeersch, T.; Hutchison, G. R. J. Cheminf. 2011, 3, 1.
- (42) Halgren, T. A. J. Comput. Chem. 1996, 17, 490-519.
- (43) O'Boyle, N. M.; Vandermeersch, T.; Flynn, C. J.; Maguire, A. R.; Hutchison, G. R. J. Cheminf. 2011, 3, 1.
- (44) Becke, A. D. J. Chem. Phys. 1993, 98, 1372-1377.
- (45) Hehre, W. J.; Ditchfield, R.; Pople, J. A. J. Chem. Phys. 1972, 56, 2257–2261.
- (46) Lee, C.; Yang, W.; Parr, R. G. Phys. Rev. B: Condens. Matter Mater. Phys. 1988, 37, 785-789.
- (47) Stephens, P. J.; Devlin, F.; Chabalowski, C. F.; Frisch, M. J. J. Phys. Chem. 1994, 98, 11623–11627.
- (48) Miertuš, S.; Scrocco, E.; Tomasi, J. Chem. Phys. 1981, 55, 117–129
- (49) Hehre, W. J.; Radom, L.; Schleyer, P. v. R. A. Ab Initio Molecular Orbital Theory; Wiley-Interscience: New York, 1986.
- (50) McQuarrie, D. A. Statistical Mechanics; Harper and Row: New York, 1975.
- (51) Casida, M. E. In *Recent Advances in Density Functional Methods*; Chong, D. P., Ed.; World Scientific: Singapore, 1995; pp 155–192.
- (52) Kendall, R. A.; Dunning, T. H.; Harrison, R. J. J. Chem. Phys. 1992, 96, 6796–6806.
- (53) Yanai, T.; Tew, D. P.; Handy, N. C. Chem. Phys. Lett. **2004**, 393, 51–57.
- (54) Crawford, T. D.; Stephens, P. J. J. Phys. Chem. A 2008, 112, 1339-1345.
- (55) Haghdani, S.; Åstrand, P.-O.; Koch, H. J. Chem. Theory Comput. **2016**, 12, 535–548.
- (56) Haghdani, S.; Hoff, B. H.; Koch, H.; Åstrand, P.-O. J. Phys. Chem. A 2017, 121, 4756-4777.
- (57) Stephens, P. J.; Harada, N. Chirality 2010, 22, 229-233.
- (58) Frisch, M. J.; Trucks, G. W.; Schlegel, H. B.; Scuseria, G. E.; Robb, M. A.; Cheeseman, J. R.; Scalmani, G.; Barone, V.; Mennucci, B.; Petersson, G. A.; Nakatsuji, H.; Caricato, M.; Li, X.; Hratchian, H. P.; Izmaylov, A. F.; Bloino, J.; Zheng, G.; Sonnenberg, J. L.; Hada, M.;

Ehara, M.; Toyota, K.; Fukuda, R.; Hasegawa, J.; Ishida, M.; Nakajima, T.; Honda, Y.; Kitao, O.; Nakai, H.; Vreven, T.; Montgomery, J. A., Jr.; Peralta, J. E.; Ogliaro, F.; Bearpark, M.; Heyd, J. J.; Brothers, E.; Kudin, K. N.; Staroverov, V. N.; Kobayashi, R.; Normand, J.; Raghavachari, K.; Rendell, A.; Burant, J. C.; Iyengar, S. S.; Tomasi, J.; Cossi, M.; Rega, N.; Millam, J. M.; Klene, M.; Knox, J. E.; Cross, J. B.; Bakken, V.; Adamo, C.; Jaramillo, J.; Gomperts, R.; Stratmann, R. E.; Yazyev, O.; Austin, A. J.; Cammi, R.; Pomelli, C.; Ochterski, J. W.; Martin, R. L.; Morokuma, K.; Zakrzewski, V. G.; Voth, G. A.; Salvador, P.; Dannenberg, J. J.; Dapprich, S.; Daniels, A. D.; Farkas, O.; Foresman, J. B.; Ortiz, J. V.; Cioslowski, J.; Fox, D. J. Gaussian 09, revision E.01; Gaussian, Inc.: Wallingford, CT, 2009.